Electronic Supplementary Material (ESI) for Journal of Materials Chemistry A.

Supplemental Information

Chemical Acronyms

Brine	saturated sodium chloride solution in water
DMF	dimethylformamide
EtOAc	ethyl acetate
HEPES	4-(2-hydroxyethyl)piperazine-ethanesulfonic acid
KOH	potassium hydroxide
MeOH	methanol
Na_2SO_4	sodium sulfate
NaH	sodium hydride
$NaBH_4$	sodium borohydride

Experimental Section

Materials

DB (99%), MDB (99%), and ferrocene (98%) were purchased from Aldrich without further purification. DBBB (99.9%, battery grade) was provided by the Materials Engineering Research Facility at Argonne National Laboratory. 23DDB, 25DDB, and 26DDB were synthesized based on the following procedures.

23DDB synthesis: NaH (880 mg, 60% dispersion in oil, 22 mmol, Sigma-Aldrich) was added in small portions to a solution of 2,3-dimethylhydroquinone (1.36 g, 10 mmol, 97%, Ark Pharm or Sigma-Aldrich) in anhydrous DMF (25 mL) under a nitrogen atmosphere. After the gas evolution had ceased, the resulting mixture was stirred at room temperature for 30 min. Iodomethane (2.49 mL, 40 mmol, 99.5%, Sigma Aldrich) was added dropwise, and the reaction mixture was stirred at 40 ^{o}C for 2 h. Saturated NaCl solution was added slowly to quench the reaction, and the resulting mixture was extracted with EtOAc. The combined organic layers were washed with water and dried over Na_2SO_4. After the solvent removal *in vacuo*, the residue was purified by flash column chromatography (silica gel, eluted with ethyl acetate/hexanes = 1/15) to yield 23DDB (1.58 g, 95%) as a white solid. ^{1}H NMR (500 MHz, $CDCl_3$) δ 6.67 (s, 2H), 3.78 (s, 6H), 2.17 (s, 6H); ^{13}C NMR (125 MHz, $CDCl_3$) δ 151.9, 126.7, 107.9, 56.1, 12.0. (Figure S4 and S5)

25DDB synthesis: $NaBH_4$ (1.13 g, 30 mmol, 98+%, Acros Organics) was added in small portions to a solution of 2,5-dimethyl-1,4-benzoquinone (2.04 g, 15 mmol, 99%, Sigma-Aldrich) in the mixture of ethanol (15 mL) and water (15 mL) under a nitrogen atmosphere. The reaction was stirred at room temperature for 30 min. A solution of

KOH (6 mL, 10 M, 60 mmol) was added, and the resulting mixture was stirred for another 30 min. Then it was heated to reflux, and dimethyl sulfate (5.70 mL, 60 mmol, ≥ 99.8%, Sigma-Aldrich) was added drop wise. The resulting mixture was stirred at reflux for 12 h before it was cooled to room temperature and extracted with EtOAc. The combined organic layers were washed with water and dried over Na_2SO_4. After concentration *in vacuo*, the residue was purified by flash column chromatography (silica gel, eluted with ethyl acetate/hexanes=1/10) to provide 25DDB (2.11 g, 85%) as a white solid. ^{1}H NMR (500 MHz, $CDCl_3$) δ 6.68 (s, 2H), 3.80 (s, 6H), 2.23 (s, 6H); ^{13}C NMR (125 MHz, $CDCl_3$) δ 151.4, 124.3, 113.7, 56.1, 16.1. (Figure S6 and S7)

26DDB synthesis: $NaBH_4$ (378 mg, 10 mmol) was added in small portions to a solution of 2,6-dimethylbenzoquinone (0.68g, 5 mmol, 99%, Sigma-Aldrich) in ethanol (5 mL) and water (5 mL) under a nitrogen atmosphere. The reaction was stirred at room temperature for 30 min. A solution of KOH (2 mL, 10 M, 20 mmol) was added, and the resulting mixture was stirred for another 30 min. Then it was heated to reflux, and dimethyl sulfate (1.89 mL, 20 mmol) was added drop wise. The resulting mixture was stirred at reflux for 12 h before it was cooled to room temperature and extracted with EtOAc. The combined organic layers were washed with water and dried over Na_2SO_4. After concentration *in vacuo*, the residue was purified by flash column chromatography (silica gel, eluted with ethyl acetate/hexanes=1/15) to provide 26DDB (0.73 g, 88%) as a colorless liquid. ^{1}H NMR (500 MHz, $CDCl_3$) δ 6.55 (s, 2H), 3.75 (s, 6H), 3.68 (s, 3H), 2.27 (s, 3H); ^{13}C NMR (125 MHz, $CDCl_3$) δ 155.3, 150.8, 131.7, 113.7, 59.9, 55.4, 16.3. (Figure S8 and S9)

Electrochemical measurements

All electrochemical experiments were performed in an argon-filled glovebox (MBraun Labmaster) at 25 °C. All electrochemical data were collected on a VMP3 potentiostat/galvanostat (Bio-Logic). All potential values were referenced to Li/Li^+. Figure S10 shows an image of the electrochemical cell used for cyclic voltammetry (CV) with the typical electrode configuration. Two different electrode combinations were used in this report. The electrochemical cell consisting of a 3 mm diameter glassy carbon (GC) working electrode (CH Instruments, Inc.), a gold coil counter electrode (CH Instruments, Inc.), and a lithium metal (Alfa Aesar) reference electrode was used for collecting the data displayed in Figures S1 and S2. For all other CV experiments, the electrochemical cell consisted of a 3 mm diameter glassy carbon working electrode (CH Instruments, Inc.), a lithium metal (Alfa Aesar) counter electrode, and a lithium metal reference electrode in a Vycor® fritted glass tube containing 0.5 M bis(trifluoromethane)sulfonimide lithium salt (LiTFSI, 99.95%, BASF) / propylene carbonate (PC, anhydrous, 99.7%, Sigma-Aldrich). The latter electrode combination is shown in Figure S10. All electrolyte solutions were dried for several days with 3 Å molecular sieves (Sigma-Aldrich). The measured water content in the electrolytes was less than 10 ppm. The glassy carbon electrode was consecutively polished on a MicroCloth™ pad with 1 μm and 0.05 μm alumina powders (Buehler), and thoroughly rinsed with deionized water after being polished with each powder. The electrode was then sonicated for 1 min in deionized water (EMD Millipore) and dried under argon before moving into the glovebox. Cell resistances were measured prior to electrochemical experiments and were ca. 250 Ω for all electrolyte solutions. As peak currents range from 0.01 to 0.1 mA depending on scan rate, additional iR contributions of ca. 2.5 to 25 mV were automatically corrected for all CV measurements using the potentiostat software. Figure S11 shows the raw and iR-corrected CV data associated with Figure 2 in the main manuscript.

Diffusion coefficients of the neutral and charged species were estimated by applying the Randles-Sevcik equation for reversible systems to the baseline corrected peak currents of the anodic and cathodic sweeps of the cyclic voltammograms, respectively:

$$|i_p| = 0.4463nFAC\left(\frac{nFD}{RT}v\right)^{\frac{1}{2}}$$

where i_p is the baseline-corrected peak current of the anodic sweep (neutral to charged) or cathodic sweep (charged to neutral) of the cyclic voltammogram (A), n is the number of electrons transferred, F is the Faraday constant (96,485 C/mol), A is the electrode area (cm^2), D is the diffusion coefficient of neutral species (Dred) or the oxidized species (Dox) (cm^2/s), v is the scan rate (V/s), C is the concentration of the neutral or the oxidized redox active compound (mol/cm^3), R is the universal gas constant (8.314 J mol^{-1} K^{-1}), and T is the temperature (K). It is important to note that the peak currents are not measured using the x-axis as a baseline. Rather, a background current baseline must first be extrapolated out to the peak potential. Then, the peak current is measured (vertically) from the peak down to the extrapolated baseline. Accordingly, the baseline corrections of the original data were performed in *MATLAB*®. Figure S12 shows a representative cyclic voltammogram with baseline corrected peak current densities indicated.

Galvanostatic cycling of different compounds was studied in 0.5 M LiTFSI / PC using a three-electrode bulk electrolysis cell (BASi) with a high surface area reticulated vitreous carbon (RVC) working electrode, a lithium metal counter electrode in a ceramic-fritted chamber with 2 mL electrolyte, and a lithium metal reference electrode in a Vycor® fritted glass tube with 0.2 mL electrolyte. The cell resistance is ca. 10 Ω as measured by the current interrupt technique. The concentration of the redox active compound was 1 mM and the total volume in the working electrolyte chamber was 30 mL. Stirring at 900 rpm in the working electrolyte chamber was maintained throughout cycling experiments. The charge / discharge current was 0.402 mA corresponding to a 0.5 C rate (so, full charge / discharge in 2 h). For 23DDB, the charge and discharge time was set for 1 h (50% state of charge) and the high cut-off voltage (charging) was set at 4.15 V and the low cut-off voltage (discharging) was set at 3.85 V, whichever was reached first. For 25DDB and DBBB, the charge and discharge time was set at 1 h (50% state of charge) and the high cut-off voltage (charging) was set at 4.10 V and the low cut-off voltage (discharging) was set at 3.80 V, whichever was reached first. The cut-off voltages were selected according to the corresponding cyclic voltammogram with *ca.* 0.15 V overpotential based on the average potential of the oxidation and the reduction peak (E^0) where for 23DDB, $E^0 \approx 4.00$ V, and for DBBB and 25DDB, $E^0 \approx 3.95$ V.

The solubility was investigated using a Dynamic Light Scattering Analyzer equipped with an optical camera and a temperature controller (0 to 70 °C, DynaPro Plate Reader II, Wyatt Technologies Co.) also located in a nitrogen-filled glovebox. The assessment was performed using the produced images of each well as a function of temperature starting from 55 °C down to 0 °C in 2.5 °C increments.

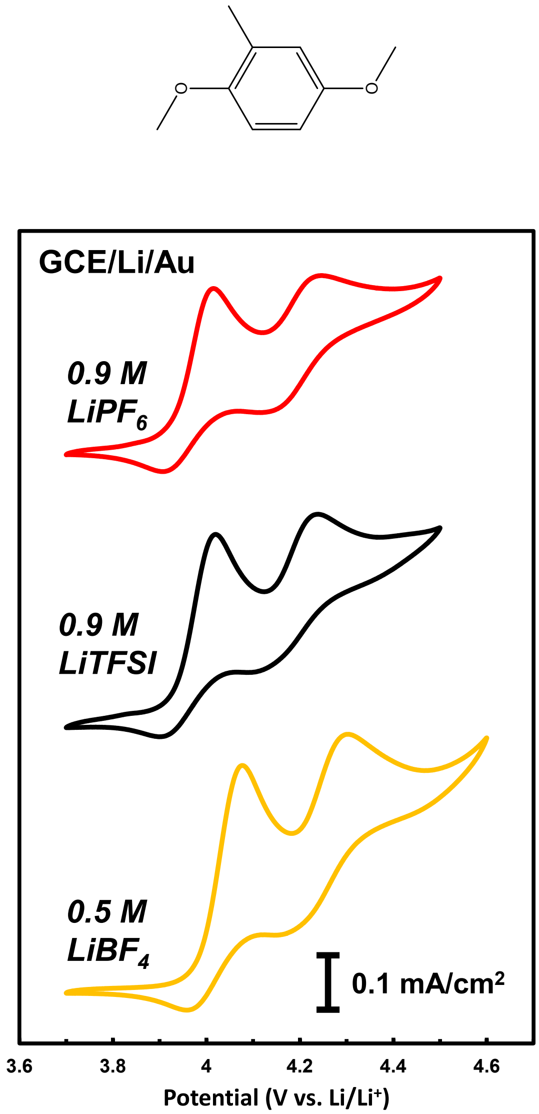

Figure S1. Cyclic voltammograms of MDB (10 mM) in PC containing different lithium salts. The working, reference, and counter electrodes are glassy carbon electrode, unfritted lithium metal, and gold coil, respectively. The scan rate is 5 mV/s.

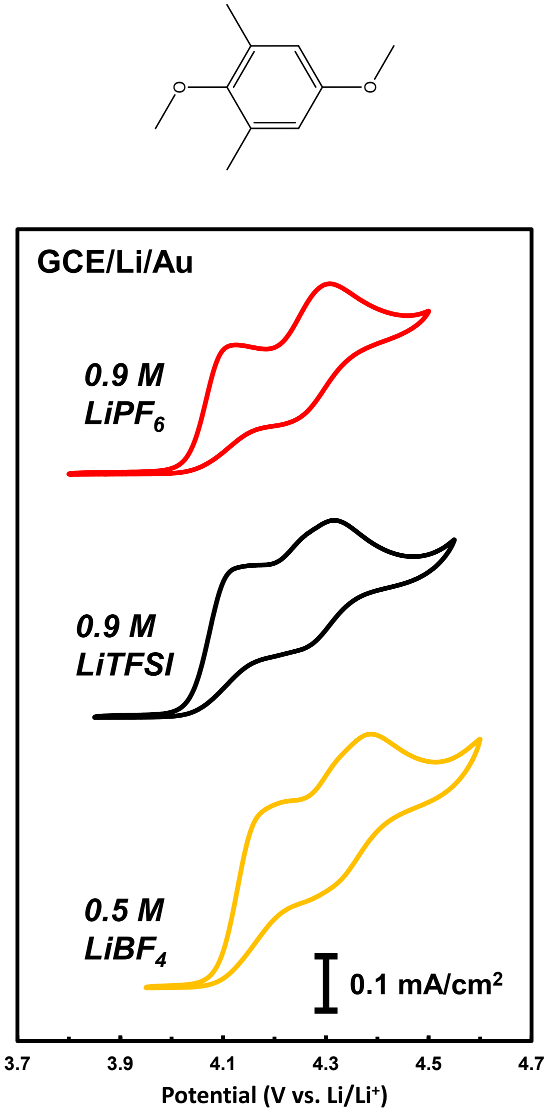

Figure S2. Cyclic voltammograms of 26DDB (10 mM) in PC containing different lithium salts. The working, reference, and counter electrodes are glassy carbon electrode, unfritted lithium metal, and gold coil, respectively. The scan rate is 5 mV/s.

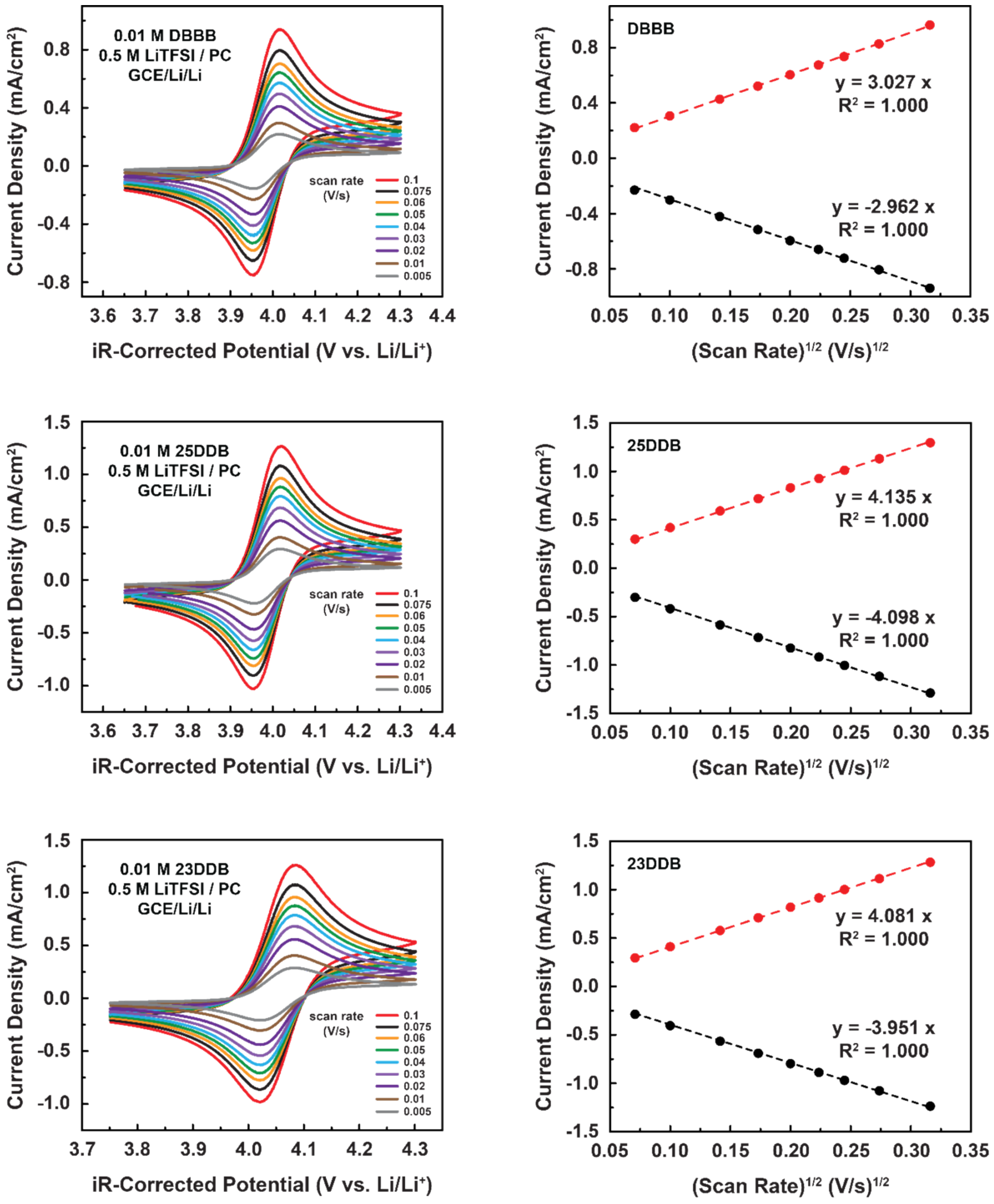

Figure S3. Cyclic voltammograms and the corresponding Randles – Sevcik plot of DBBB, 25DDB, and 23DDB. All electrolytes consist of 10 mM active species in 0.5 M LiTFSI / PC. The working, reference, and counter electrodes are glassy carbon electrode, fritted lithium metal, and unfritted lithium metal, respectively.

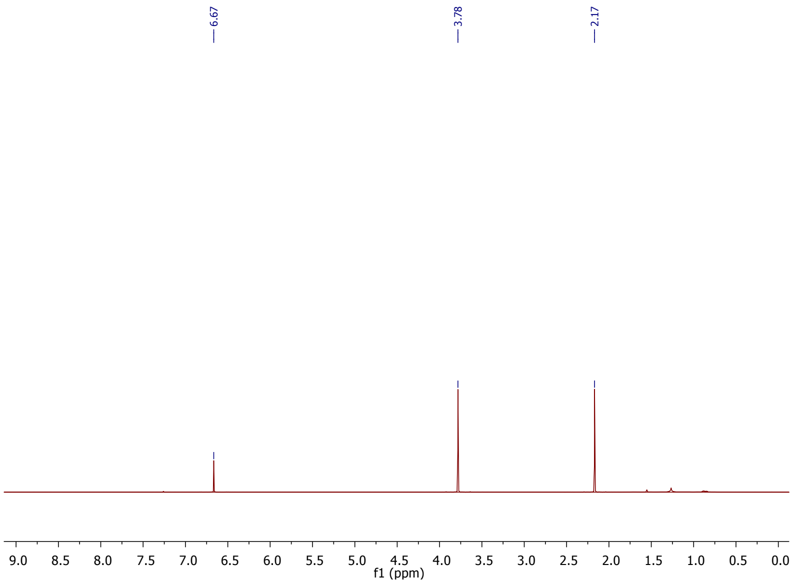

Figure S4. ^{1}H NMR of 23DDB

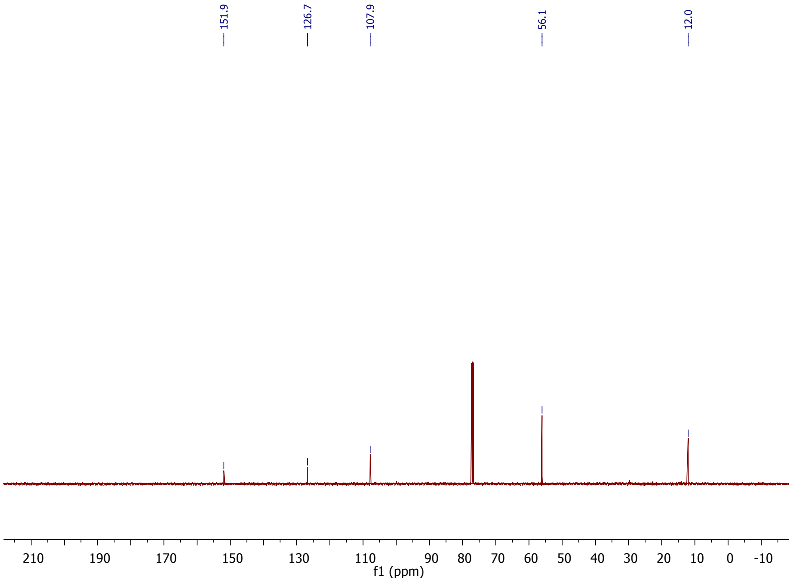

Figure S5. ^{13}C NMR of 23DDB

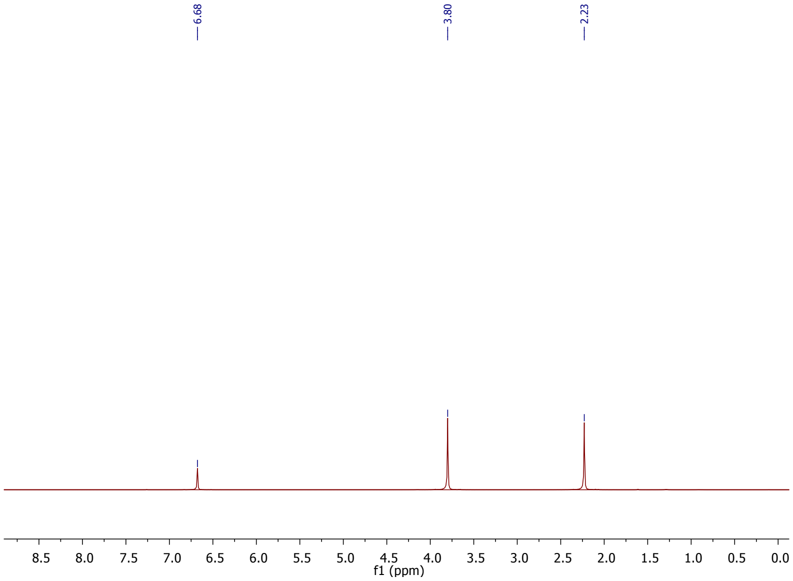

Figure S6. ^{1}H NMR of 25DDB

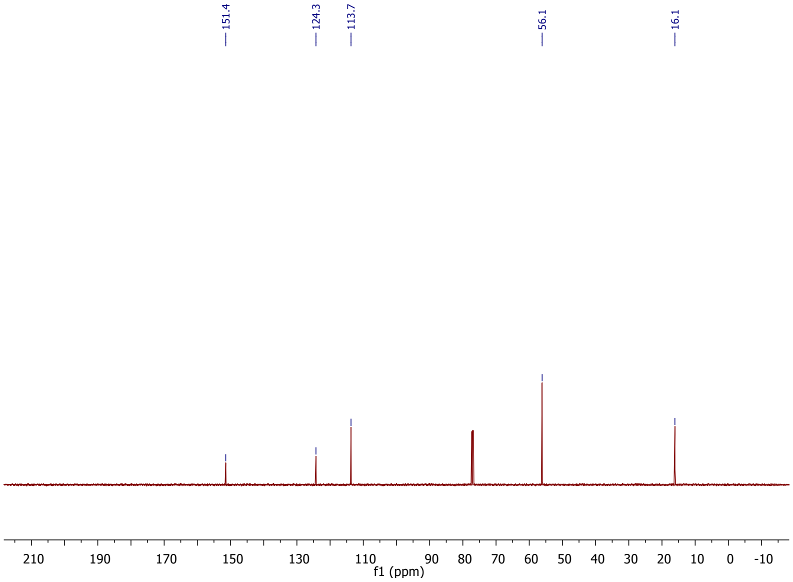

Figure S7. ^{13}C NMR of 25DDB

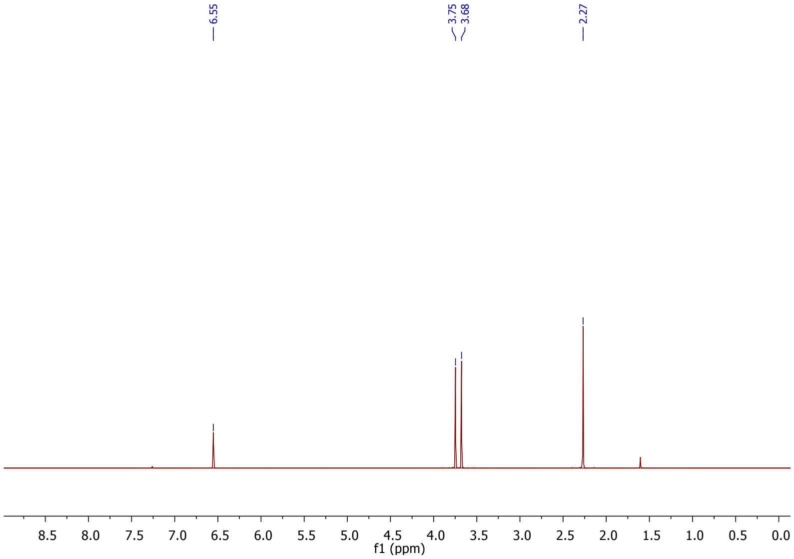

Figure S8. ^{1}H NMR of 26DDB

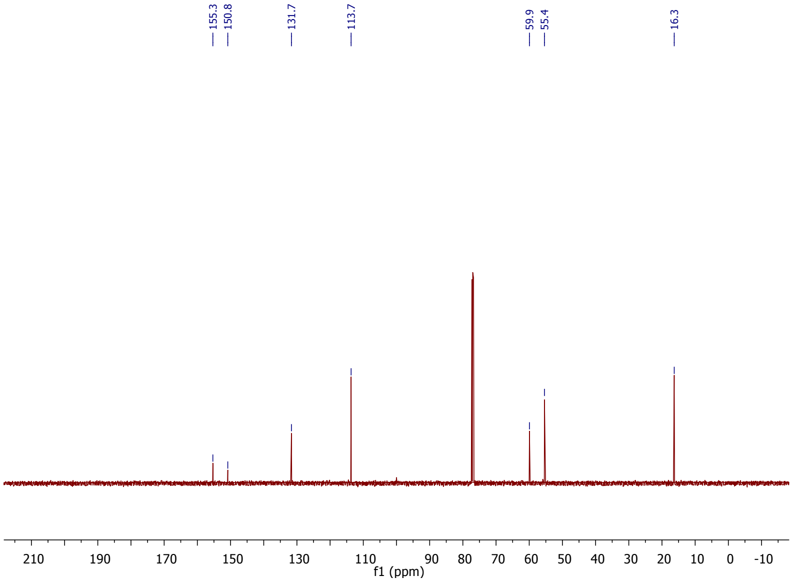

Figure S9. ^{13}C NMR of 26DDB

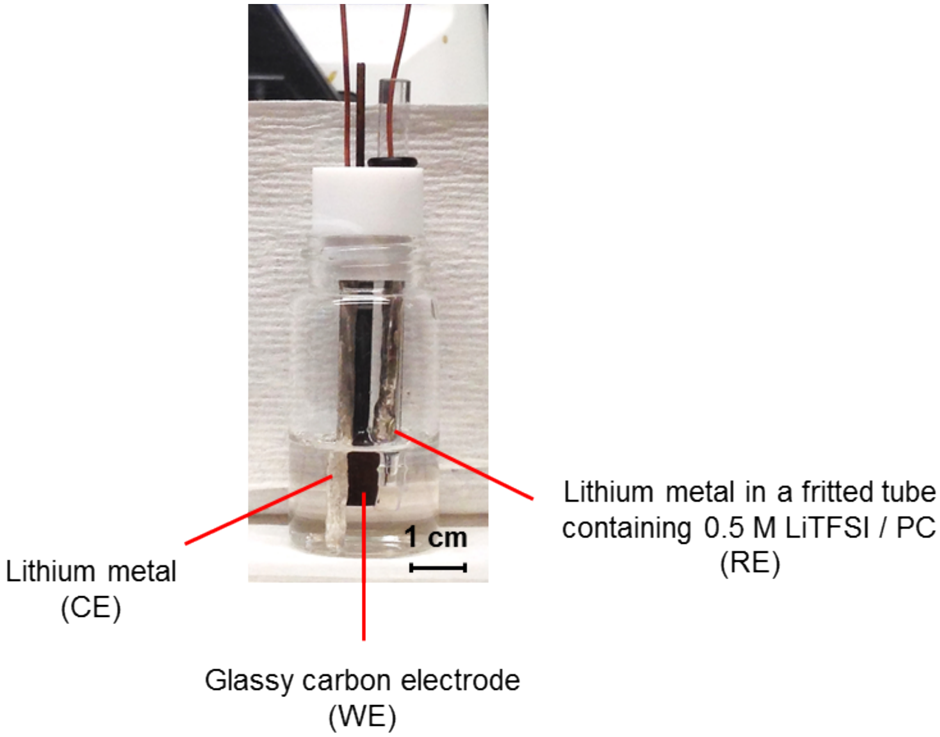

Figure S10. A digital photograph of the electrochemical cell used for the cyclic voltammetry measurements in the main text. WE, CE, and RE stand for working electrode, counter electrode, and reference electrode.

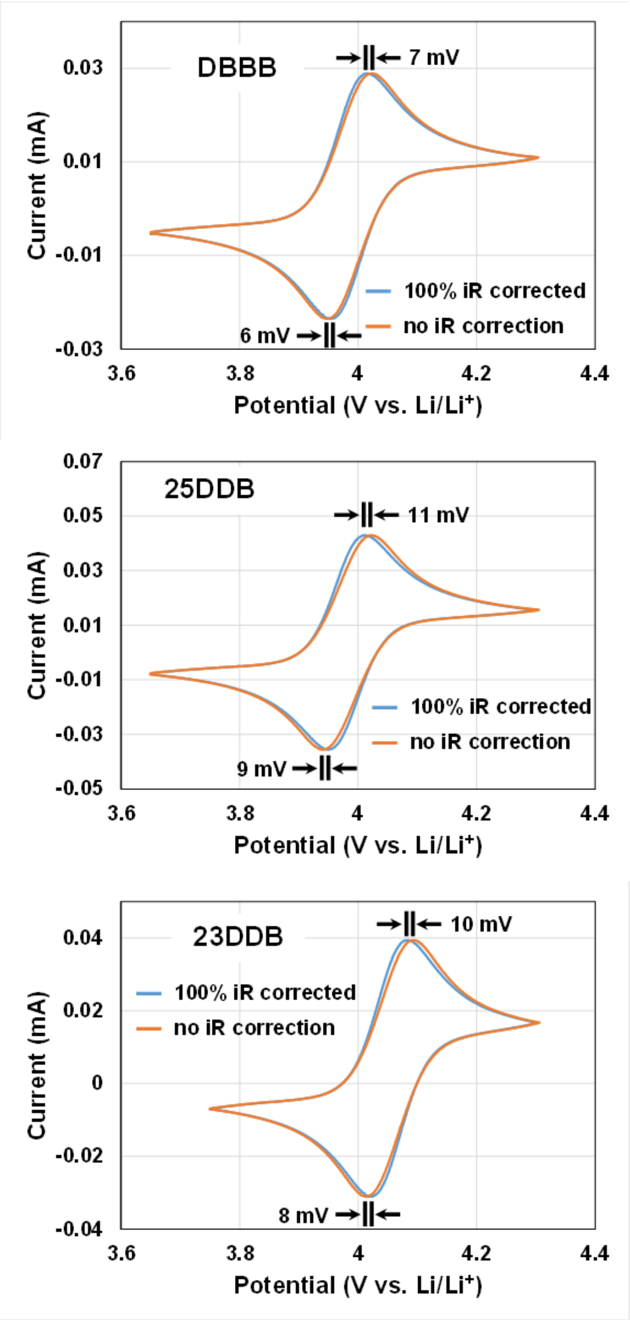

Figure S11. Raw and iR-corrected cyclic voltammograms of 2,5-di-*tert*-butyl-1,4-bis(2-methoxyethoxy)benzene (DBBB), 2,5-dimethyl-1,4-dimethoxybenzene (25DDB) and 2,3-dimethyl-1,4-dimethoxybenzene (23DBB), shown in Figure 2 in the main text. All electrolytes consisted of 10 mM active species in 0.5 M LiTFSI / PC. The working, reference, and counter electrodes are glassy carbon electrode, fritted lithium metal, and unfritted lithium metal, respectively. The scan rate is 0.02 V/s.

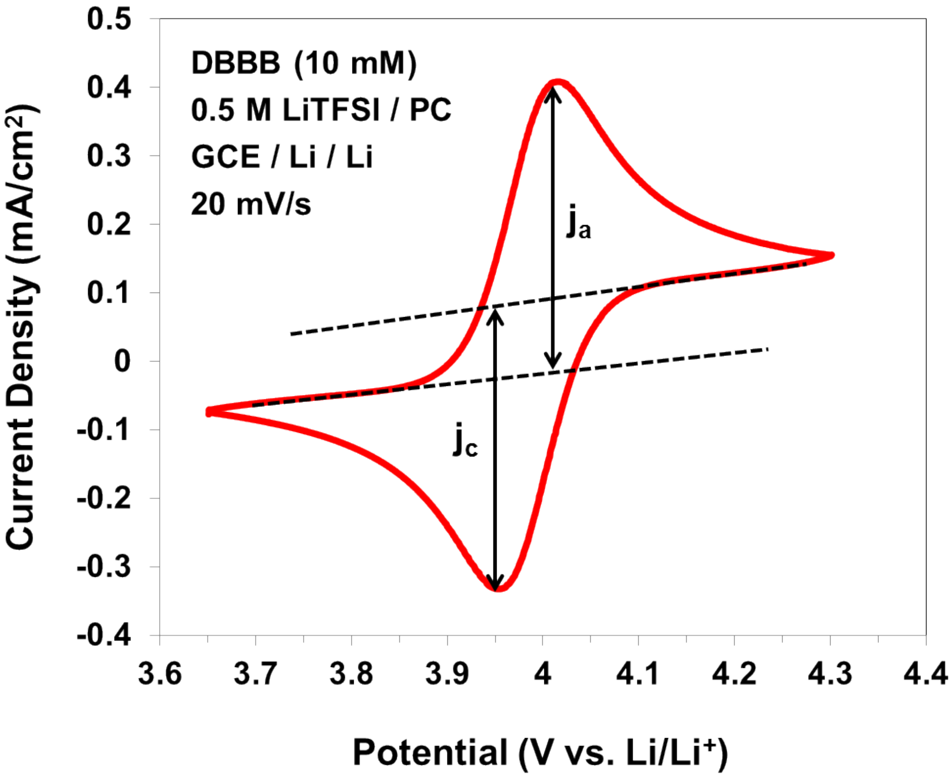

Figure S12. Representative cyclic voltammogram of 2,5-di-*tert*-butyl-1,4-bis(2-methoxyethoxy)benzene (DBBB) with baseline corrected peak current densities indicate for the anodic and cathodic sweeps of the voltammogram. The electrolyte consisted of 10 mM DBBB in 0.5 M LiTFSI / PC. The working, reference, and counter electrodes are glassy carbon electrode, fritted lithium metal, and unfritted lithium metal, respectively. The scan rate is 0.02 V/s.